transmitochondrial lines obtained by injection of CAP23 mitochondria into either $\rho^0$206 or 143B had low respiratory competence.

The variation in respiratory competence observed among sets of transformants obtained with different mitochondrial donors did not correlate with the number of mtDNA molecules per cell in the transformants (Table 1), nor did the striking deviation in respiratory capacity of an occasional cell line within each group. This intragroup variability in respiratory competence probably reflects variation among the individual recipient cells. Yet, the possibility that heterogeneity in the exogenous mtDNA population may have contributed to the observed variability in respiratory phenotype among transformants obtained by injection of individual organelles cannot be excluded.

Our results show that ρ^0 human cells can be repopulated with exogenous human mitochondria and restored to respiratory competence. Cell lines differing only in their mtDNA genotype—that is, the parental 143B.TK$^-$ cell line and the various groups of transformants containing mitochondria from HT1080, HeLa S3, HeLaBU25 10B3R, or CAP23 cells—exhibited respiratory differences. The sequence diversity of human mtDNA and of the mtDNA of these cell lines (*12*) is probably responsible for differences in respiratory capacity. A comparison of the respiratory capacities of the various sets of transmitochondrial cell lines with those of the mtDNA donors indicates that nuclear background also affects the respiratory competence of a cell.

The genetic analysis of mitochondrial biogenesis applied to *Saccharomyces cerevisiae* (*1*) can now be extended to mammalian cells. Thus, it should be possible to select for nuclear suppressors of mtDNA mutations affecting mitochondrial function, or conversely, for mtDNA suppressors of mutations of nuclear genes controlling mitochondrial biogenesis.

Our work is also relevant to the study of mitochondrial neuromuscular diseases (*13*). In several cases, specific mtDNA mutations have been associated with these diseases (*14*). Our results suggest that one possible mechanism for the observed different degrees of penetrance of these diseases is the existence of specific interactions of the variable complements of nuclear genes present in different individuals with a mitochondrial genome containing a mutation. Introduction of mitochondria derived from patients affected with these disorders into ρ^0 cells may help distinguish whether a defect is mtDNA- or nuclear DNA–encoded. Furthermore, repopulation of ρ^0 cells by microinjection of single organelles could be used to clone the mutant mitochondrial genome from a heteroplasmic population.

REFERENCES AND NOTES

1. G. Attardi and G. Schatz, *Annu. Rev. Cell Biol.* **4**, 289 (1988).
2. M. P. King and G. Attardi, in preparation.
3. P. Desjardins *et al.*, *Mol. Cell. Biol.* **5**, 1163 (1985); P. Desjardins *et al.*, *Somatic Cell Mol. Genet.* **12**, 133 (1986); R. Morais *et al.*, *In Vitro Cell. Dev. Biol.* **24**, 649 (1988).
4. M. Grégoire *et al.*, *Eur. J. Biochem.* **142**, 49 (1984).
5. C. M. Croce, *Proc. Natl. Acad. Sci. U.S.A.* **73**, 3248 (1976).
6. M. P. King and G. Attardi, *Cell* **52**, 811 (1988).
7. T. T. Puck *et al.*, *J. Exp. Med.* **103**, 273 (1956).
8. J. Masters, B. Keeley, H. Gay, G. Attardi, *Mol. Cell. Biol.* **2**, 498 (1982). The 10B3R, originally a methotrexate-resistant derivative of HeLa BU25, has been grown for an extended time in the absence of methotrexate and has lost the amplified copies of the dihydrofolate reductase gene.
9. C. H. Mitchell, J. M. England, G. Attardi, *Somatic Cell Genet.* **1**, 215 (1975).
10. Dot blot analyses were carried out on 50- to 100-μl samples of cell suspensions containing 5×10^4 cells, which were brought to 1 ml with 50 m*M* tris, *p*H 8 (25°C), 10 m*M* EDTA, 100 m*M* NaCl, digested overnight at 50°C with 250 μg of proteinase K, and incubated with 0.5*M* NaOH at 37°C for 16 hours to hydrolyze RNA [G. Attardi, H. Parnas, M.-I. H. Hwang, B. Attardi, *J. Mol. Biol.* **20**, 145 (1966)]. A standard curve was constructed with known amounts of closed circular or Bam HI–digested HeLa mtDNA mixed with samples of 5×10^4 143B206 cells digested and alkali-treated as described above. The mtDNA clone mp18.XH5.2, containing the 1237-bp Xba I–Hind III fragment of HeLa mtDNA [2204-7441; S. Anderson *et al.*, *Nature* **290**, 457 (1981)] cloned into Xba I + Hind III double-digested M13mp18, was labeled by extension of the universal primer and used as probe [H. M. Sucov *et al.*, *Dev. Biol.* **44**, 47 (1987)]. Our values for mtDNA for the parental cell lines were lower than those previously reported (*6*), because of the more complete removal of RNA by alkali digestion in our experiments.
11. A. Wiseman and G. Attardi, *Mol. & Gen. Genet.* **186**, 364 (1982).
12. Cann *et al.* [R. L. Cann, M. Stoneking, A. C. Wilson, *Nature* **325**, 31 (1987)] estimated that the mtDNA sequence diversity between random individuals is 0.32%. From a survey of ~7% of the mitochondrial genome with ten restriction enzymes, we have found an approximately 0.3% difference in the mtDNA nucleotide sequence between HeLa S3 and 143B.TK$^-$ and between 143B.TK$^-$ and HT1080 and a 0.5% difference between HeLa S3 and HT1080, in substantial agreement with the above estimate. The mtDNAs of HeLa S3, HeLaBU25 10B3R, and CAP23 are closely related.
13. S. DiMauro *et al.*, *Ann. Neurol.* **17**, 521 (1985); J. A. Morgan-Hughes, *Trends Neurosci.* **2**, 15 (1986); R. A. Capaldi, *Trends Biochem. Sci.* **13**, 144 (1988); D. C. Wallace, *Trends Genet.* **5**, 9 (1989).
14. I. J. Holt *et al.*, *Nature* **331**, 717 (1988); M. Zeviani *et al.*, *Neurology* **38**, 1339 (1988); D. C. Wallace *et al.*, *Science* **242**, 1427 (1988).
15. G. E. Veomett, in *Techniques in Somatic Cell Genetics*, J. W. Shay, Ed. (Plenum, New York, 1982), pp. 67–79.
16. T. H. Norwood and C. J. Zeigler, *ibid.*, pp. 35–45.
17. Y. Nakamura *et al.*, *Science* **235**, 1616 (1987); Y. Nakamura *et al.*, *Nucleic Acids Res.* **15**, 10073 (1987).

18. Supported by NIH grant GM11726. We thank S. Lai for carrying out the cytochrome c oxidase assays, B. Keeley for determining growth curves, P. C. Gaines of the Caltech Microchemical Facility for the extraction of DNA samples, J. Houldsworth and our colleagues in the laboratory for reading the manuscript, and A. Drew and L. Tefo for technical help.

24 April 1989; accepted 28 August 1989

Myristoylated and Nonmyristoylated Forms of a Protein Are Phosphorylated by Protein Kinase C

JONATHAN M. GRAFF, JEFFREY I. GORDON, PERRY J. BLACKSHEAR*

Activation of protein kinase C is thought to require association of the kinase with the cell membrane. It has been assumed that cellular substrates for the kinase must likewise be associated with membranes, and previous studies with membrane-associated myristoylated proteins have supported this view. It is now shown that a mutation that prevents the normal amino-terminal myristoylation of a prominent cellular substrate of protein kinase C, and appears to prevent its membrane association, does not prevent the normal phosphorylation of this protein in intact cells in response to phorbol esters. Thus, membrane association may not be required in order for protein kinase C substrates to undergo phosphorylation.

PROTEIN KINASE C (PKC), THE DIacylglycerol-activated, Ca^{2+}- and phospholipid-dependent protein kinase, has been implicated in the regulation of many cellular processes (*1*). Because the kinase requires lipid cofactors for activation, it is thought to exist in an active form only in close proximity to the cell membrane (*2, 3*). In addition, most cellular substrates for PKC are thought to be either integral membrane proteins or associated with the membrane in other ways (*3*). One example of such a substrate is pp60$^{v\text{-}src}$, in which NH_2-terminal myristoylation promotes membrane association (*4–6*); a mutation that

J. M. Graff and P. J. Blackshear, Howard Hughes Medical Institute Laboratories, Durham, NC 27710, and the Section of Diabetes and Metabolism, Division of Endocrinology, Metabolism, and Genetics, Departments of Medicine and Biochemistry, Duke University Medical Center, Durham, NC 27710.
J. I. Gordon, Departments of Biochemistry and Molecular Biophysics, and Medicine, Washington University School of Medicine, St. Louis, MO 63110.

*To whom correspondence should be addressed.

Table 1. In vitro myristoylation of NH_2-terminal MARCKS peptides. The wild-type (GAQFSKTA) and mutant (AAQFSKTA) MARCKS peptides and two peptides of known affinity derived from the NH_2-termini of the catalytic subunit of cAMP-dependent protein kinase (GNAAAARR) and cytochrome b_5 reductase (GAQLSTLG) were used as substrates for NMT in an in vitro assay system (*17, 18*). All peptides were assayed in three independent experiments and the means of these values are shown; the interassay variation was less than 15%. V_{max} data are reported as a percentage of the velocity observed with the cAMP-dependent protein kinase octapeptide.

Peptide	K_m (μM)	V_{max} (%)	V_{max}/K_m
GNAAAARR*	60	100	1.7
GAQLSTLG†	3	23	7.7
GAQFSKTA	0.12	2.5	20.8
AAQFSKTA	ND‡	ND	

*See (*17*). †See (*14*). ‡ND indicates that myristoylation of the peptide had an undetectable velocity (V_{max} was <1%).

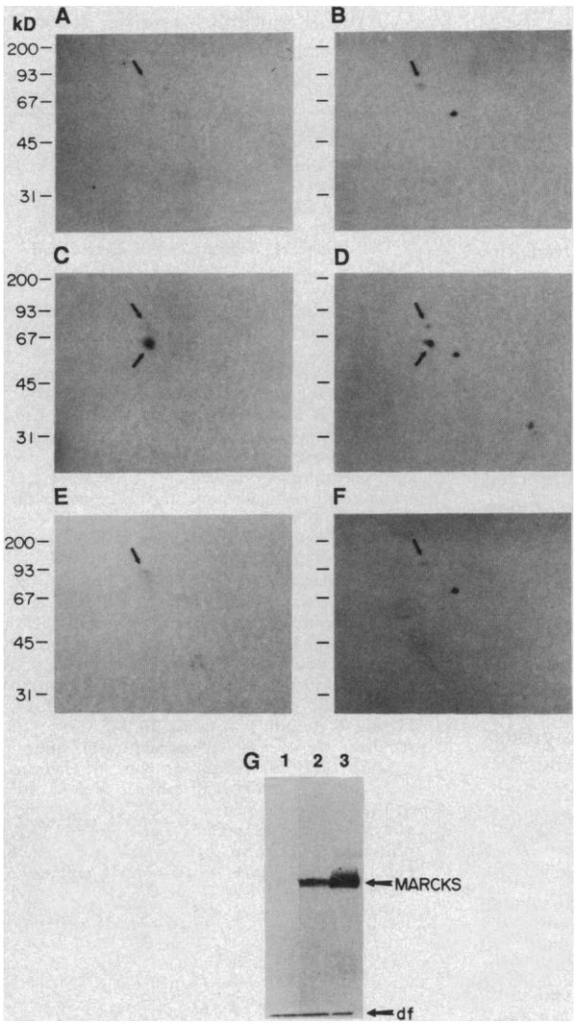

Fig. 1. Expression and [^{3}H]myristate-labeling of wild-type and mutant chicken MARCKS proteins in COS cells. COS cells were transfected with (**A** and **B**) the expression vector alone or the vector encoding (**C** and **D**) the wild-type or (**E** and **F**) mutant MARCKS protein as described (*11, 12*). The cells were labeled for 4 hours with [9,10-^{3}H(N)]myristate (Du Pont, Biotechnology Systems; 0.3 mCi/ml) and then fractionated into (A, C, and E) supernatant and (B, D, and F) particulate fractions (*6*). Equal amounts of trichloroacetic acid–precipitatable radioactivity from these cellular fractions were separated by two-dimensional gel electrophoresis (*23*); the gels were treated with Enhance (Du Pont Biotechnology Systems) and subjected to autoradiography. The position of the endogenous monkey MARCKS protein is indicated by the arrow pointing down; the position of the chicken MARCKS protein is indicated by the arrow pointing up; the positions of molecular mass standards are indicated. (**G**) An immunoblot, performed as described (*24*), in which each lane was loaded with equal amounts of trichloroacetic acid–precipitable radioactivity from supernatant fractions from the same [^{3}H]myristate-labeled COS cells described in (A) to (F). These cells were transfected with (lane 1) vector alone or the vector expressing (lane 2) the wild-type or (lane 3) mutant MARCKS protein. The arrows indicate the positions of the immunoreactive chicken MARCKS proteins with molecular masses of ~67 kD and the gel dye front (df). The rabbit antiserum was raised to purified chicken MARCKS protein (*22, 24*); this antiserum does not cross-react with MARCKS proteins from several mammalian species tested. The nonmyristoylated mutant protein migrates with the same apparent molecular mass as the normal chicken protein.

prevents myristoylation of the protein also prevents its association with the membrane and its ability to serve as a substrate for PKC (*6*). We now show that a mutation preventing the myristoylation of a cellular substrate for PKC did not affect its ability to undergo phosphorylation by PKC in intact cells. Thus, in contrast to the tyrosine kinase $pp60^{v\text{-}src}$, myristoylation and consequent membrane association do not appear to be absolute requirements for phosphorylation of this substrate by PKC.

The protein evaluated in this study is a prominent cellular substrate for PKC, frequently referred to as the 80- to 87-kD protein because of its characteristic migration on SDS-polyacrylamide gels (*7*). This protein appears to be a direct substrate for PKC, not only in cell-free systems but also in a variety of intact cells (*3, 7–9*). Although approximately 40% of the protein was found to be associated with a synaptosomal membrane fraction from brain (*8*), most studies in cultured cells have determined that the protein is predominantly cytosolic (*9*). In murine macrophages, the protein was found to be myristoylated (*10*), a modification that might be expected to affect the association of the protein with lipid membrane components. We recently predicted the primary sequences of both the bovine and chicken proteins from cloning and cDNA sequence analysis (*11, 12*); because their predicted molecular masses differed markedly from those calculated from SDS-polyacrylamide gels, and for other reasons, we suggested the name myristoylated alanine-rich C-kinase substrate (MARCKS) for these proteins. We also found that the NH_2-terminal 14 amino acids were identical in the chicken and bovine proteins, although the identity between the entire proteins was only 65%. Excluding the initiator Met, the NH_2-terminus of both proteins contained the sequence GAQFSKTA (*13*), which conforms to the proposed consensus sequence for myristoylation and contains the required NH_2-terminal Gly residue (*11, 12, 14–16*). However, there were no other regions of the primary sequence, such as hydrophobic domains, that might predispose the MARCKS proteins to associate preferentially with membranes (*11, 12*).

We first assessed the ability of two synthetic peptides to serve as substrates for *N*-myristoyl transferase (NMT). The first corresponded to the NH_2-terminal eight residues of the normal protein without the initiator Met, and the second was identical except for the conservative substitution of Ala for the NH_2-terminal Gly. These octapeptides were characterized in an in vitro myristoylation assay, which has been used to characterize the peptide and fatty acyl coenzyme A substrate specificities of yeast and mammalian NMT (*15, 17, 18*). The NH_2-terminal MARCKS octapeptide GAQFSKTA was a good substrate for NMT (Table 1); the enzyme exhibited a high affinity for this peptide relative to another well-characterized octapeptide derived from the NH_2-terminal sequence (GNAAAARR) of a known myristoylated protein, the catalytic subunit of the adenosine 3′,5′-monophosphate (cAMP)–dependent protein kinase (*18*). The catalytic efficiency [maximal velocity (V_{max}) divided by the Michaelis constant (K_m)] of NMT for the MARCKS octapeptide was 12 times as great as that of the cAMP-dependent protein kinase octapeptide. The NH_2-terminal sequence of the MARCKS protein resembles the NH_2-terminal sequence of another known myristoylated protein, cytochrome b_5 reductase (GAQLSTLG) (*19*). The cata-

lytic efficiency of NMT for the MARCKS octapeptide was also better than that for a peptide spanning residues 2 to 9 of this enzyme (Table 1). As expected, substitution of an NH_2-terminal Ala for Gly in the MARCKS octapeptide prevented it from serving as a substrate for NMT (Table 1).

We constructed a plasmid in which the Gly^2 of the chicken MARCKS protein (*11*) was replaced with an Ala by in vitro mutagenesis. On the basis of the in vitro data, this conservative change should produce a mutant MARCKS protein that is not a substrate for NMT. The wild-type and the mutant chicken MARCKS sequences were cloned into the expression vector pBC12-CMV (*20*), which we have used to express the chicken protein in mammalian cells (*11*). We transfected COS cells with either the wild-type or mutant plasmids, incubated the cells for 4 hours with [^{3}H]myristate, and then fractionated them (*6*) into cytosolic and particulate components. The wild-type MARCKS protein was myristoylated, whereas the mutant MARCKS protein was not; that the mutant protein was expressed to a comparable extent was demonstrated by immunoblotting with an antiserum specific for the chicken protein (Fig. 1).

To determine whether the mutant MARCKS protein could still serve as a substrate for PKC in intact cells, we transfected COS cells with either the wild-type or the mutant MARCKS plasmids, incubated the cells with ^{32}P-labeled inorganic phosphate, and exposed them for 15 min to 1.6 μ*M* 12-*O*-tetradecanoyl phorbol-13-acetate (TPA) or vehicle. Under these conditions, TPA causes most cellular PKC activity to become associated with the cellular particulate components; however, no increase in cytosolic Ca^{2+}- and phospholipid-independent histone IIIS kinase activity (protein kinase M) was noted after TPA treatment (*21*). In COS cells, TPA stimulated the phosphorylation of both the wild-type and the mutant proteins (Fig. 2). Similar results were obtained after transfecting the plasmids into mouse L cells (*21*).

To determine whether the sites phosphorylated by PKC were similar in the mutant and wild-type proteins, we compared tryptic phosphopeptide maps of the phosphorylated MARCKS proteins isolated from TPA-stimulated COS cells transfected with either the wild-type or nonmyristoylated mutant constructions. The phosphorylated MARCKS proteins were isolated by two-dimensional gel electrophoresis, localized by autoradiography, and digested with trypsin. Analysis of the phosphopeptides by reversed-phase high-performance liquid chromatography (HPLC) showed that the wild-type and mutant MARCKS proteins were phosphorylated on similar or identical sites (Fig. 3), which have been shown to be the sites phosphorylated by PKC (*22*).

Finally, to assess whether myristoylation played a role in the association of the MARCKS protein with the cellular membranes, we compared the subcellular distribution of the wild-type and nonmyristoylated mutant MARCKS proteins. Transfected COS cells were incubated with ^{32}P-labeled inorganic phosphate, exposed to TPA or vehicle, and then fractionated into cytosolic and particulate components as described for the $pp60^{v\text{-}src}$ proteins (*6*), and the radioactivity incorporated into the MARCKS proteins in each fraction was quantitated. Both the myristoylated chicken and monkey proteins associated to a greater extent with the particulate fraction than did the nonmyristoylated mutant chicken protein, which was almost completely cytosolic (Table 2). Similar studies using immunoblot analysis showed that more than 95% of the immunoreactive mutant protein partitioned into the crude cytosolic fraction (*21*).

We conclude that the TPA-stimulated, PKC-mediated phosphorylation of the MARCKS proteins was similar for both myristoylated and nonmyristoylated forms.

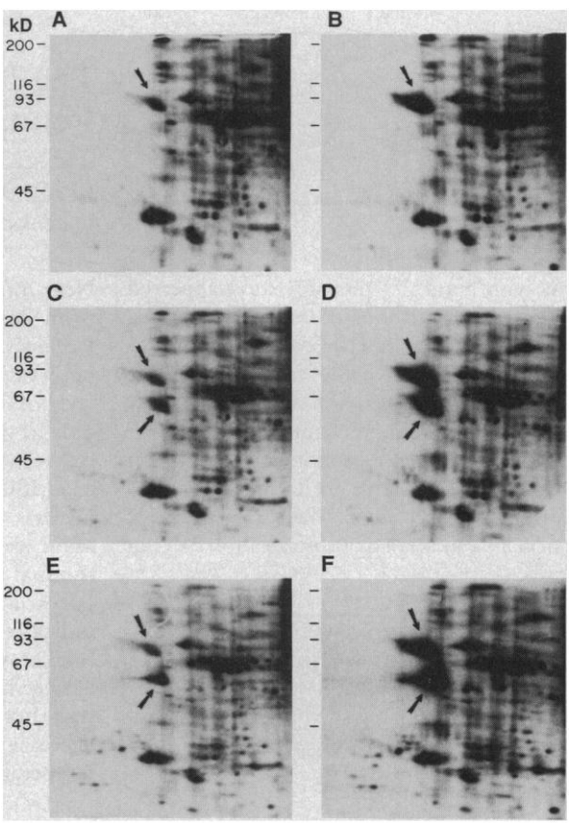

Fig. 2. Phosphorylation of the wild-type and mutant chicken MARCKS proteins in COS cells. COS cells were transfected with (**A** and **B**) the expression vector alone, or the vectors expressing the (**C** and **D**) wild-type or (**E** and **F**) mutant MARCKS proteins as described (*11*). The cells were incubated with ^{32}P-labeled inorganic phosphate and then exposed to (A, C, and E) control conditions (0.01% dimethyl sulfoxide) or (B, D, and F) TPA (1.6 μ*M* in 0.01% dimethyl sulfoxide) for 15 min. Equal amounts of trichloroacetic acid–precipitable radioactivity from the total cell lysate were subjected to two-dimensional gel electrophoresis and autoradiography (*23*). The position of the endogenous monkey MARCKS protein is indicated by the arrows pointing down; the positions of the (C and D) wild-type or (E and F) mutant chicken MARCKS proteins are indicated by the arrows pointing up. The positions of the molecular mass standards are indicated.

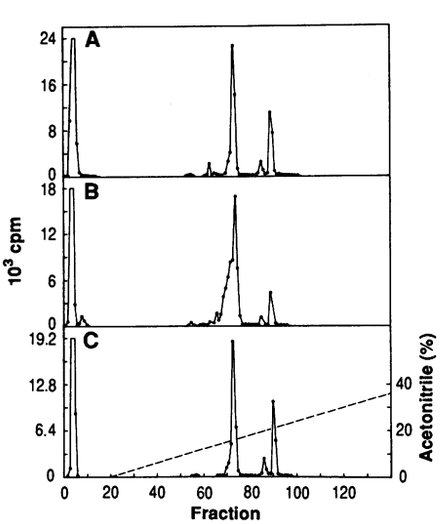

Fig. 3. Tryptic phosphopeptide maps of the transfected wild-type chicken, mutant chicken, and endogenous monkey MARCKS proteins. COS cells were transfected with the wild-type or mutant chicken MARCKS plasmids, incubated with ^{32}P-labeled inorganic phosphate, and exposed to TPA (*22*). The ^{32}P-labeled (**A**) wild-type, (**B**) mutant, or (**C**) endogenous monkey, MARCKS proteins were localized by autoradiography, excised from the gel, and digested with trypsin, and the tryptic digests of the ^{32}P-labeled proteins were separated on a C4 reversed-phase HPLC column with a linear gradient of acetonitrile (dashed line) (*22*). Fractions (0.2 ml) were collected at 1-min intervals and the radioactivity of each fraction was determined by Cerenkov scintillation counting. The identities of the phosphopeptide peaks have been described (*22*); the large peak eluting in the isocratic portion of the gradient represents a specific phosphopeptide.

Table 2. Subcellular localization of normal and mutant MARCKS proteins. COS cells were transfected with plasmid constructs, incubated with ^{32}P-labeled inorganic phosphate, and exposed to control conditions or TPA (Fig. 2). The cells were then fractionated into crude cytosol and particulate fractions (*6*). The ^{32}P-labeled MARCKS proteins were identified on two-dimensional gels by autoradiography, and the spots were excised and counted in Biofluor (Du Pont, Biotechnology Systems). Results are shown as the cytosolic radioactivity in MARCKS expressed as a percentage of the cytosolic plus particulate radioactivity in MARCKS; the values are from two separate experiments (1 and 2).

Treatment	Cytosolic radioactivity (%)		
	Endogenous monkey	Normal chicken	Mutant chicken
Control			
1	39	42	90
2	45	62	94
TPA			
1	43	69	96
2	75	71	100

As with pp60$^{v\text{-}src}$, myristoylation appeared to increase membrane association of the MARCKS protein. However, in contrast to pp60$^{v\text{-}src}$, in which a Gly^2 to Ala^2 nonmyristoylated mutant was not a substrate for PKC in intact cells (*6*), the mutated MARCKS protein could be phosphorylated readily on exposure of the cells to TPA. Our results suggest the possibility that truly cytosolic proteins can serve as substrates for PKC in cells.

REFERENCES AND NOTES

1. Y. Nishizuka, *Science* **233**, 305 (1986).
2. R. M. Bell, *Cell* **45**, 631 (1986).
3. J. R. Woodgett, T. Hunter, K. L. Gould, in *Cell Membranes: Methods and Reviews*, E. L. Elson, W. A. Frazier, L. Glazer, Eds. (Plenum, New York, 1987), pp. 215–340.
4. D. Pellman, E. A. Garber, F. R. Cross, H. Hanafusa, *Nature* **314**, 374 (1985).
5. F. R. Cross, E. A. Garber, D. Pellman, H. Hanafusa, *Mol. Cell. Biol.* **4**, 1834 (1984).
6. J. E. Buss, M. R. Kamps, K. Gould, B. M. Sefton, *J. Virol.* **58**, 468 (1986).
7. J. E. Niedel and P. J. Blackshear, in *Phosphoinositides and Receptor Mechanisms*, J. W. Putney, Ed. (Liss, New York, 1986), pp. 47–88; A. Rodriguez-Pena and E. Rozengurt, *EMBO J.* **4**, 71 (1985); P. J. Blackshear, L. Wen, B. P. Glynn, L. A. Witters, *J. Biol. Chem.* **261**, 1459 (1986); C. M. Isacke *et al.*, *EMBO J.* **5**, 2889 (1986); A. Rodriguez-Pena and E. Rozengurt, *ibid.*, p. 77; P. J. Blackshear, D. J. Stumpo, J.-K. Huang, R. A. Nemenoff, D. H. Spach, *J. Biol. Chem.* **262**, 7774 (1987).
8. K. A. Albert, S. I. Walaas, J. K. T. Wang, P. Greengard, *Proc. Natl. Acad. Sci. U.S.A.* **83**, 2822 (1986).
9. P. J. Blackshear, L. A. Witters, P. R. Girard, J. F. Kuo, S. N. Quamo, *J. Biol. Chem.* **260**, 13304 (1985).
10. A. A. Aderem *et al.*, *Nature* **332**, 362 (1988).
11. J. M. Graff, D. J. Stumpo, P. J. Blackshear, *Mol. Endocrinol.*, in press.
12. D. J. Stumpo, J. M. Graff, K. A. Albert, P. Greengard, P. J. Blackshear, *Proc. Natl. Acad. Sci. U.S.A.* **86**, 4012 (1989).
13. Abbreviations for the amino acid residues are as follows: A, Ala; C, Cys; D, Asp; E, Glu; F, Phe; G, Gly; H, His; I, Ile; K, Lys; L, Leu; M, Met; N, Asn; P, Pro; Q, Gln; R, Arg; S, Ser; T, Thr; V, Val; W, Trp; and Y, Tyr.
14. D. A. Towler *et al.*, *Proc. Natl. Acad. Sci. U.S.A.* **84**, 2708 (1987).
15. D. A. Towler *et al.*, *J. Biol. Chem.* **263**, 1784 (1988).
16. D. A. Towler, J. I. Gordon, S. P. Adams, L. Glaser, *Annu. Rev. Biochem.* **57**, 69 (1988).
17. D. A. Towler and L. Glaser, *Proc. Natl. Acad. Sci. U.S.A.* **83**, 2812 (1986).
18. D. A. Towler, S. R. Eubanks, D. S. Towery, S. P. Adams, L. Glaser, *J. Biol. Chem.* **262**, 1030 (1987).
19. J. Ozols, S. A. Carr, P. Strittmater, *ibid.* **259**, 13349 (1984).
20. B. R. Cullen, *Cell* **46**, 973 (1986).
21. J. M. Graff, D. M. Haupt, P. J. Blackshear, unpublished data.
22. J. M. Graff, D. J. Stumpo, P. J. Blackshear, *J. Biol. Chem.* **264**, 11912 (1989).
23. D. H. Spach, R. A. Nemenoff, P. J. Blackshear, *ibid.* **261**, 12750 (1986).
24. J. M. Graff, T. N. Young, J. D. Johnson, P. J. Blackshear, *J. Biol. Chem.*, in press.

25. We thank R. R. Randall, M. McAdams, and K. Theisen for synthesis of oligonucleotides, D. M. Haupt and E. Jackson-Machelski for technical assistance, and S. Cotecchia for helpful discussions. Supported in part by grants from the NIH (2T32-GM-07171, AI27179), the Howard Hughes Medical Institute Graduate Student Support Fund, and Monsanto Company. J.I.G. is an Established Investigator of the American Heart Association and P.J.B. is an Investigator of the Howard Hughes Medical Institute.

4 May 1989; accepted 29 August 1989

The Nature of the Near-Infrared Features on the Venus Night Side

D. CRISP, W. M. SINTON, K.-W. HODAPP, B. RAGENT, F. GERBAULT, J. H. GOEBEL, R. G. PROBST, D. A. ALLEN, K. PIERCE, K. R. STAPELFELDT

Near-infrared images of the Venus night side show bright contrast features that move from east to west, in the direction of the cloud-top atmospheric superrotation. Recently acquired images of the Venus night side along with earlier spectroscopic observations allow identification of the mechanisms that produce these features, their level of formation, and the wind velocities at those levels. The features are detectable only at wavelengths near 1.74 and 2.3 micrometers, in narrow atmospheric windows between the CO_2 and H_2O bands. The brightest features have brightness temperatures near 480 Kelvin, whereas the darkest features are more than 50 Kelvin cooler. Several factors suggest that this radiation is emitted by hot gases at altitudes below 35 kilometers in the Venus atmosphere. The feature contrasts are produced as this thermal radiation passes through a higher, cooler, atmospheric layer that has horizontal variations in transparency. The 6.5-day east-west rotation period of the features indicates that equatorial wind speeds are near 70 meters per second in this upper layer. Similar wind speeds have been measured by entry probes and balloons at altitudes between 50 and 55 kilometers in the middle cloud layer. The bright features indicate that there are partial clearings in this cloud deck. The presence of these clearings could decrease the efficiency of the atmospheric greenhouse that maintains the high surface temperatures on Venus.

ALLEN AND CRAWFORD (*1*) USED A single-channel near-infrared (NIR) photometer at the Anglo-Australian Observatory 3.9-m telescope to produce the first maps of the Venus night side at wavelengths between 1 and 5 μm. Their images revealed bright features that moved from east to west across the night side, in the direction of the cloud-top 4-day wind (*2*). Simultaneous spectroscopic observations showed that this emission was most intense in narrow spectral regions centered near 1.74 and 2.3 μm. In this report, we describe results of a new ground-based observing program that was designed to identify the mechanisms that produce these features, determine their level of formation in the Venus atmosphere, and measure the wind velocities at those levels.

We conducted a coordinated NIR imaging program at Kitt Peak (1.3-m telescope) and Mauna Kea (University of Hawaii 2.2-m telescope) observatories during May and June of 1988, before and after Venus passed through inferior conjunction. NIR array cameras were used to collect hundreds of

D. Crisp, Jet Propulsion Laboratory, California Institute of Technology, Pasadena, CA 91109.
W. M. Sinton and K.-W. Hodapp, Institute for Astronomy, University of Hawaii, Honolulu, HI 96822.
B. Ragent, San Jose State University Foundation, San Jose, CA 95192.
F. Gerbault, Sterling Software, National Aeronautics and Space Administration (NASA), Ames Research Center, Moffett Field, CA 94035.
J. H. Goebel, NASA Ames Research Center, Moffett Field, CA 94035.
R. G. Probst, Kitt Peak National Observatory, Tucson, AZ 85726.
D. A. Allen, Anglo-Australian Observatory, Epping, NSW, Australia.
K. Pierce and K. R. Stapelfeldt, California Institute of Technology, Pasadena, CA 91125.